

The crystal structure of takéuchiite, $\text{Mg}_{1.71}\text{Mn}_{1.29}\text{BO}_5$ A combined single crystal X-ray and HRTEM study

R. Norrestam and J.-O. Bovin*

Structural Chemistry Group, Chemistry Department B, DTH 301,
The Technical University of Denmark, DK-2800 Lyngby, Denmark

Received: May 13, 1987

*Single crystal structure / X-ray diffraction / Electron microscopy /
Mineral / Metal oxyborate*

Abstract. Crystals of the mineral takéuchiite, $\text{Mg}_{1.59}\text{Mn}_{1.20}\text{Fe}_{0.19}\text{BO}_5$ were investigated by X-ray diffraction and high resolution electron microscopy (HREM) techniques. The space group is *Pnmm*, $Z = 24$, with the unit cell dimensions $a = 27.585(4)$, $b = 12.561(3)$ and $c = 6.027(2)$ Å. The structural model previously derived from HREM studies was refined versus the 1492 most significant X-ray reflections to an *R* value of 0.063. The crystal structure can be interpreted as a chemical twinning of the basic structure type pinakiolite. As for other members of this structural family some of the cation positions are disordered.

Introduction

The mineral takéuchiite, M_3BO_5 ($\text{Mg}_{1.59}\text{Mn}_{1.20}\text{Fe}_{0.19}\text{Ti}_{0.01}\text{BO}_5$), was found in a specimen from Långban mine, Sweden (Bovin and O'Keeffe, 1980). A preliminary crystal structure was derived by matching experimentally obtained high-resolution transmission electron microscope (HRTEM) images with computed ones. The structure was described as a chemical twinning (Andersson and Hyde, 1974) of the parent structure of pinakiolite (Moore and Araki, 1974) and is thus closely related to the other known chemical twins of pinakiolite, viz. ludwigite (Takéuchi et al., 1950) and orthopinakiolite (Takéuchi et al., 1978).

* *Permanent address:* National Center for HREM, Chemical Center, University of Lund, P.O. Box 124, S-22100 Lund, Sweden.

The aim of the present investigation was to obtain the accurate crystal structure of takéuchiite by means of single crystal X-ray diffraction using the metal atom positions derived from the HRTEM investigation to initiate the solution.

Experimental

A crystalline specimen of the mineral was kindly put to our disposal by the Swedish Museum of National History (specimen No. R 332376).

X-ray diffraction studies

A selected single crystal was initially studied by conventional photographic X-ray diffraction techniques. The indicated possible space groups $Pnmm$ and $Pnn2$ confirmed the earlier observations by Bovin and O'Keeffe (1980). From measurements on a single crystal diffractometer the unit cell parameters were determined at 293(1) K to $a = 27.585(4)$, $b = 12.561(3)$ and $c = 6.027(2)$ Å. With the schematic formula M_3BO_5 the number of formula units per unit cell is 24. Single crystal X-ray diffraction data were registered at 293(1) K using graphite-monochromatized $MoK\alpha$ radiation and a scintillation detector with pulse height discrimination. The intensity data collected with the ω - 2θ scan technique (scan interval $1.0 + 0.35 \tan\theta$) were corrected for background, Lorentz, polarization and absorption effects. Further experimental conditions are given in Table 1.

In related complex borate structures of wall paper type (Moore and Araki, 1974), the shortest unit translation is about 3 Å. The shortest translation of the present structure is 6.027(2) Å and indicates a deviation from an ideal symmetry. This is apparently due to uneven distributions of distorted coordination polyhedra and of metal occupancies in the structure. As a consequence, reflections with l odd are generally much weaker than those with l even, which will in combination with the limited crystal sizes imply practical limitations on the possibilities of collecting an extensive set of significant reflections. The 1492 most significant unique reflections, used for the structure refinements, were collected with $MoK\alpha$ radiation up to a θ angle of 35° and correspond to 47% of the possible reflections with l even and 20% of those with l odd. Within the low angle ($< 20^\circ$) part of this data set, 68% of the possible reflections with l even and 45% of those with l odd were present.

HREM studies

Micrographs were taken using Philips EM 430 and Jeol 200 CX transmission electron microscopes, both with a resolving power of 2.3 Å. The crystals were prepared for the HRTEM study in the same way as described

Table 1. Experimental conditions for the crystal structure determination of takéuchiite.

Crystal shape	Prismatic
Crystal size	0.09 × 0.15 × 0.23 mm
Diffractometer	Enraf-Nonius CAD4
Determination of unit cell:	
Number of reflections used	13
θ -range	10.0 to 15.8°
Intensity data collection:	
Maximum $\sin(\theta)/\lambda$	0.800 Å ⁻¹
Range of h , k and l	0 to 22, 0 to 19 and 0 to 7
Standard reflections	(004) and (1840)
Intensity instability	< 3%
Number of unique reflections	4278
Number of observed reflections	1492
Criterion for significance	$I > 5 \sigma(I)$
Absorption correction:	
Linear absorption coefficient	48.1 cm ⁻¹
Transmission factor range	0.48 to 0.65
Structure determination technique	Model derived from electron micrographs
Structure refinement:	
Minimization of	Sum of $w\Delta F^2$
Isotropic thermal parameters	All atoms
Number of refined parameters	142
Weighting scheme	$1/\sigma(F)^2$
Final R	0.063
Final wR	0.067
Final max shift/sigma	0.3
Final max and min in $\Delta\rho$	5.1 and $-1.9 \text{ e}^- \cdot \text{Å}^{-3}$

before (Bovin et al., 1981). Calculated images from the structural parameters of the X-ray diffraction work were produced using the multislice method with a local version of the program SHRLI.

Structure determination and refinement

The metal atom positions, for space group symmetry $Pnmm$, suggested by Bovin et al. (1981) from a comparison between experimental and computed electron microscope images (cf. Fig. 1), were used as the starting point of the crystal structure determination. Electron micrographs recorded along the b axis (cf. Fig. 2) revealed that no crystals studied showed disorder in the c axis direction. To overcome the pseudosymmetry of the initial structural model for the metal atoms, the number of refined parameters was increased very slowly in the first stages of refinement. By successively

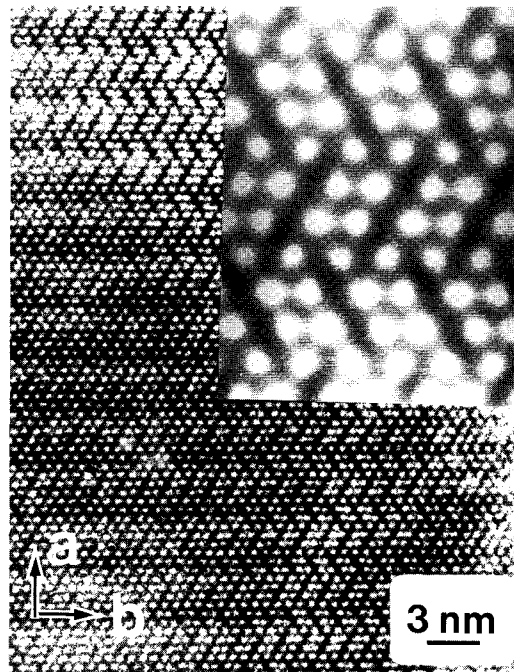


Fig. 1. Electron micrograph of a well ordered takéuchiite crystal, recorded with the electron beam parallel to the c axis. A simulated image, computed from the initial atomic parameters, is inserted. White contrast represents the boron atom positions in the structure (cf. Fig. 3).

increasing the number of parameters, the preliminary model eventually included coordinates, isotropic thermal and occupancy factors of each metal atom. The occupancies used, describe the fractional occupancy of Mn and Mg at each position (with their sum fixed to unity). Oxygen atoms were located from difference electron density ($\Delta\rho$) maps and boron atoms from geometrical considerations. As it is difficult to differentiate between Fe^{3+} and Mn^{3+} in an X-ray diffraction study, the Fe^{3+} content is treated as Mn^{3+} throughout the present investigation.

To achieve a reasonable convergence of the least-squares refinements for the present rather complex structure, with its large extent of pseudosymmetry and partial substitutional disorder, the model was kept as simple as possible. Thus, the corresponding atoms in each pair of the borate groups, related by the pseudotranslation $(0,0,\frac{1}{2})$, were constrained to have identical x and y coordinates. All the atoms in such related pairs of borate groups were assumed to have a common isotropic thermal parameter. The metal positions, for which the fractional occupancies refined to values not

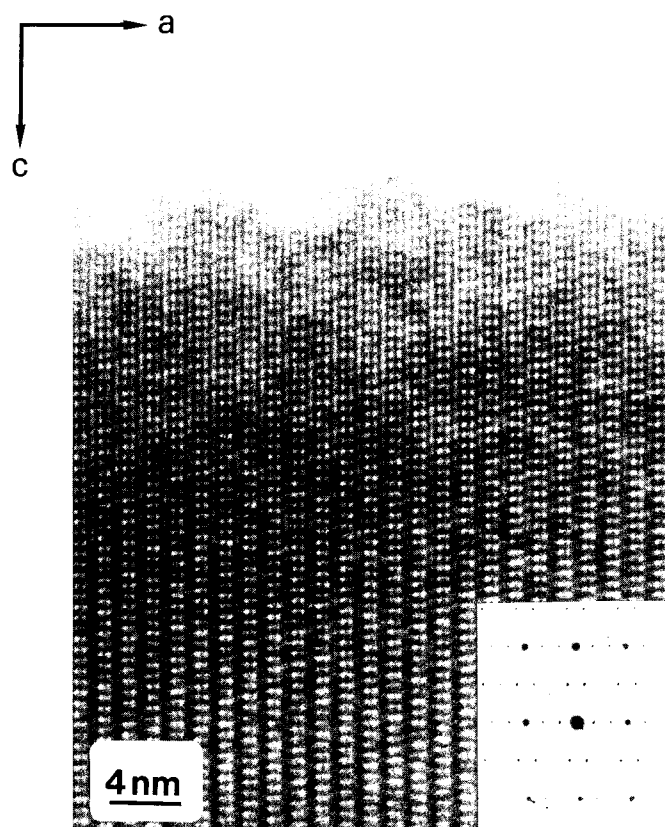


Fig. 2. Electron micrograph of a takéuchiite crystal, recorded with the electron beam parallel to the *b* axis. A selected area diffraction pattern is inserted showing the ordered *c* axis.

significantly different from unity for Mn or Mg, were given fixed fractional occupancies of 1.0. Attempts to lower the space group symmetry to $Pnn2$ at this stage were unsuccessful and yielded a poorer convergence especially for the intensities of reflections with *l* odd. Accordingly, the space group $Pnmm$ was adopted for the final least-squares treatments.

During the refinements and subsequent $\Delta\varrho$ calculations, it became evident that the M2 position was disordered around the twofold position $(0, \frac{1}{2}, \frac{1}{2})$. The two prominent peaks with almost equal heights, found in a $\Delta\varrho$ map calculated without any M2 contribution (cf. Fig. 8), could be properly approximated by allowing M2 to occupy a fourfold position $(x, y, \frac{1}{2})$ with a fractional occupancy of 0.5. This disorder model gives rise to e.g. abnormal metal-metal distances (1.186 Å) between M2 and the adjoining M7 atom,

Table 2. Fractional atomic coordinates ($\times 10^4$) and refined isotropic thermal parameters ($\times 10^4 \text{ \AA}^2$) of takéuchiite. The temperature factor expression used was $\exp(-8\pi^2 U \sin^2 \theta / \lambda^2)$.

Atom	%Mn	x	y	z	U
m(1)	16(2)	0	0	2483(16)	53(15)
m(2)	42(6)	476(4)	4821(9)	0	165(34)
m(3)	100	0	5000	5000	33(8)
m(4)	18(2)	-33(2)	2773(3)	2477(13)	55(11)
m(5)	11(2)	1683(2)	5079(3)	2489(15)	56(11)
m(6)	6(2)	1626(2)	640(3)	2529(13)	62(12)
m(7)	0	763(4)	4118(8)	0	215(22)
m(8)	100	834(2)	3880(3)	5000	42(6)
m(9)	31(3)	1589(3)	2876(6)	0	192(20)
m(10)	100	1697(2)	2867(3)	5000	34(6)
m(11)	43(3)	2524(2)	1692(5)	0	42(15)
m(12)	100	2523(2)	1696(4)	5000	54(8)
m(13)	20(2)	3317(2)	2872(3)	2513(12)	41(9)
m(14)	100	4164(2)	3933(4)	0	42(6)
m(15)	100	4163(2)	3922(4)	5000	35(6)
o(1)		-396(3)	1383(7)	2477(30)	60(16)
o(2)		1278(4)	-765(6)	2504(31)	69(19)
o(3)		1318(4)	3602(7)	2814(22)	69(21)
o(4)		2963(4)	1460(7)	2584(31)	87(20)
o(5)		4643(4)	-777(7)	2168(21)	62(21)
o(6)		2037(4)	2085(7)	2724(22)	67(19)
o(7)		466(4)	2364(7)	0	72(9)
o(8)		466(4)	2364(7)	5000	72(9)
o(9)		466(4)	462(7)	0	72(9)
o(10)		466(4)	462(7)	5000	72(9)
o(11)		1221(3)	1389(7)	0	72(9)
o(12)		1221(3)	1389(7)	5000	72(9)
o(13)		3810(4)	503(7)	0	75(9)
o(14)		3810(4)	503(7)	5000	75(9)
o(15)		4551(4)	1513(7)	0	75(9)
o(16)		4551(4)	1513(7)	5000	75(9)
o(17)		3789(4)	2398(7)	0	75(9)
o(18)		3789(4)	2398(7)	5000	75(9)
o(19)		2837(4)	3330(7)	0	98(11)
o(20)		2837(4)	3330(7)	5000	98(11)
o(21)		2099(4)	4351(7)	0	98(11)
o(22)		2099(4)	4351(7)	5000	98(11)
o(23)		2872(4)	5232(7)	0	98(11)
o(24)		2872(4)	5232(7)	5000	98(11)
b(1)		717(5)	1425(10)	0	72(9)
b(2)		717(5)	1425(10)	5000	72(9)
b(3)		4053(5)	1463(11)	0	75(9)
b(4)		4053(5)	1463(11)	5000	75(9)
b(5)		2606(6)	4297(11)	0	98(11)
b(6)		2606(6)	4297(11)	5000	98(11)

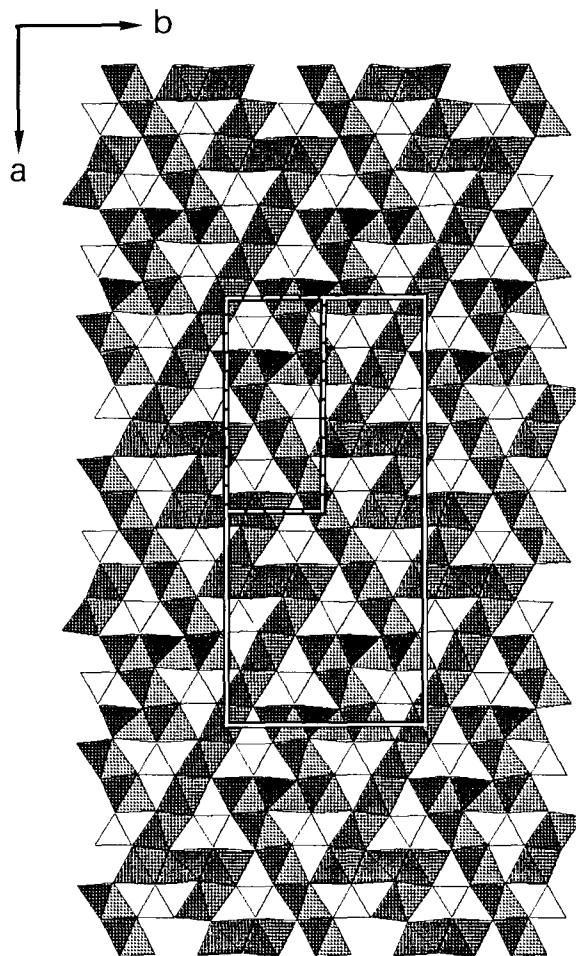


Fig. 3. Polyhedral drawing of the takéuchiite structure viewed along the c axis, showing the zig-zag and the flat walls (C and F walls respectively) of edge-sharing octahedra. The unit cell is outlined with the fundamental unit (cf. Fig. 4) indicated by broken lines. The borate groups are represented by small triangles.

and thus this part of the structure remains somewhat undetermined. A further discussion on the origin and nature of this disorder is given below.

Further details on the final structural refinement are given in Table 1. The atomic coordinates and occupancies are listed in Table 2. The coordination polyhedra around each metal ion as well as the labelling of the ions are shown in Figures 3 and 4. The Guinier X-ray powder pattern as calculated from the observed single crystal X-ray diffraction intensities is

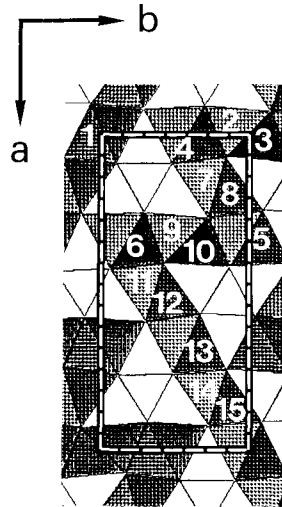


Fig. 4. The fundamental unit (cf. Fig. 3) in the takéuchiite structure viewed along the c axis. Labels on the different coordination octahedra are in accordance with the metal labelling given in Table 2. In case of two labels for one octahedra position, the upper left one is given for metal atoms at $z = 0$ and the lower right one for atoms at $z = 0.5$.

Table 3. Powder pattern of takéuchiite calculated from the observed single crystal X-ray diffraction intensities.

d value	I_c	h	k	l	d value	I_c	h	k	l
6.0452	6	4	1	0	2.0332	59	9	2	2
5.8881	7	1	0	1	1.9950	11	8	3	2
5.7159	23	2	2	0	1.9357	18	10	2	2
5.3315	9	1	1	1	1.9118	24	9	3	2
5.1862	78	3	2	0	1.6428	13	11	4	2
3.0135	24	0	0	2	1.5797	27	12	4	2
2.7545	12	9	2	0	1.5344	10	14	3	2
2.7291	36	5	4	0	1.5230	25	15	2	2
2.5931	57	6	4	0	1.5206	40	3	7	2
2.5279	19	4	2	2	1.5067	26	0	0	4
2.5204	100	6	0	2	1.4699	14	15	3	2
2.4559	14	7	4	0	1.3773	12	18	4	0
2.3515	12	7	1	2	1.3028	18	6	4	4
2.2330	19	8	1	2	1.1494	13	24	0	0
2.2046	27	6	5	0					

listed in Table 3. It should be noted that the mineral specimen contains contaminations of other materials than takéuchiite. Thus, a calculated pattern representing pure takéuchiite appears valuable for i.a. identification purposes.

Table 4. Percentage Mn, metal-oxygen bond distance (e.s.d.'s about 0.01 Å) and multiplicity in the coordination polyhedra of takéuchiite, $\text{Mg}_{1.71}\text{Mn}_{1.29}\text{BO}_5$.

16	M1—O1	2.053	2	31	M9—O3	2.066	2
	—O9	2.056	2		—O6	2.283	2
	—O10	2.071	2		—O11	2.126	1
					—O21	2.325	1
42	M2—O5	1.893	4	100	M10—O3	1.918	2
	—O16	2.268	2		—O6	1.931	2
100	M3—O5	1.906	4		—O12	2.273	1
	—O15	2.268	2		—O22	2.169	1
18	M4—O1	2.013	1	43	M11—O4	1.994	2
	—O5	2.126	1		—O6	2.177	2
	—O7	2.094	1		—O19	2.231	1
	—O8	2.113	1		—O24	2.134	1
	—O15	2.106	1	100	M12—O4	1.918	2
	—O16	2.087	1		—O6	1.979	2
11	M5—O3	2.120	1		—O20	2.227	1
	—O4	1.992	1		—O23	2.138	1
	—O13	2.104	1	20	M13—O2	2.044	1
	—O14	2.094	1		—O4	2.025	1
	—O21	2.098	1		—O17	2.084	1
	—O22	2.108	1		—O18	2.073	1
6	M6—O2	2.010	1		—O19	2.092	1
	—O6	2.143	1		—O20	2.081	1
	—O11	2.111	1	100	M14—O1	1.985	2
	—O12	2.086	1		—O2	1.972	2
	—O23	2.097	1		—O10	2.175	1
	—O24	2.122	1		—O17	2.187	1
0	M7—O3	2.375	2	100	M15—O1	1.963	2
	—O5	2.045	2		—O2	1.977	2
	—O7	2.351	1		—O9	2.188	1
	—O14	2.100	1		—O18	2.174	1
100	M8—O3	1.908	2				
	—O5	1.904	2				
	—O8	2.159	1				
	—O13	2.261	1				

Table 5. Short (< 3.0 Å) metal-metal distances (Å) in takéuchiite.

M1—M1	2.993
M3—M8	2.698
M4—M4	2.986
M6—M6	2.979
M7—M9	2.762
M8—M10	2.698
M9—M11	2.976
M10—M12	2.713

The structural refinements were carried out by means of the SHELX-76 package (Sheldrick, 1976), using atomic scattering factors from International Tables for X-ray Crystallography (1974). The polyhedral packing diagrams were obtained by means of the computer graphics program POLY (Norrestam, 1984)¹.

Discussion

The general structural features are in agreement with the description given earlier by Takéuchi (1978), when predicting this structure type. As shown in Figure 3, the structure is composed of trigonal BO_3 groups and of metal ions coordinated octahedrally by oxygen ions. The octahedra share corners and edges, giving rise to zig-zag and flat walls (denoted C and F walls by Takéuchi, 1978) extending along the c direction (cf. Fig. 3). Similar types of arrangements have been found in related transition metal borates as pinakiolite, ludwigite and orthopinakiolite (see e.g. Moore and Araki, 1974; Takéuchi et al., 1950, 1978). The takéuchiite structure can be derived from the parent structure of pinakiolite (Bovin et al., 1981a) by using the concept of chemical twinning (Andersson and Hyde, 1974).

The columns along c , formed by the coordination polyhedra around M4, M5 and M6 (denoted S columns by Takéuchi, 1978), have a dominant Mg^{2+} content, 82, 89 and 94% Mg respectively. This is in accordance with the occupancies found in the related metal positions of pinakiolite and orthopinakiolite. Each of these octahedra have one significantly shorter (about 2.0 Å) metal oxygen bond and five longer ones (about 2.1 Å). The oxygen atoms involved in the shorter bonds are those shared between the S columns and the flat F wall. The same arrangement applied for the octahedra around M4, M5 and M6 in the present structure (cf. Fig. 4).

The flat F wall is shown in Figure 5 together with the labels of the metal ions in the columns of octahedra forming the wall. The results from the crystal structure analysis of pinakiolite and orthopinakiolite, suggesting that the metal content in every second column in the F wall should be dominated by Mg^{2+} , is confirmed by the present study. Thus, the Mg^{2+} content in the central column in the wall with metal ions M1 is 84%, the next nearest column with ions M13 is 80% and the last column with ions M6 is 94%. The metal-oxygen bonds in the octahedra around M6 has been discussed above, as M6 can also be considered as forming an S column. In the octahedra around M1 and M13, the metal-oxygen distances are rather constant, as expected for the rather undistorted coordination polyhedra usually observed around Mg^{2+} , with an average of about 2.06 Å. The

¹ Additional material to this paper can be ordered referring to the no. CSD 52598, names of the authors and citation of the paper at the Fachinformationszentrum Energie, Physik, Mathematik GmbH, D-7514 Eggenstein-Leopoldshafen 2, FRG.

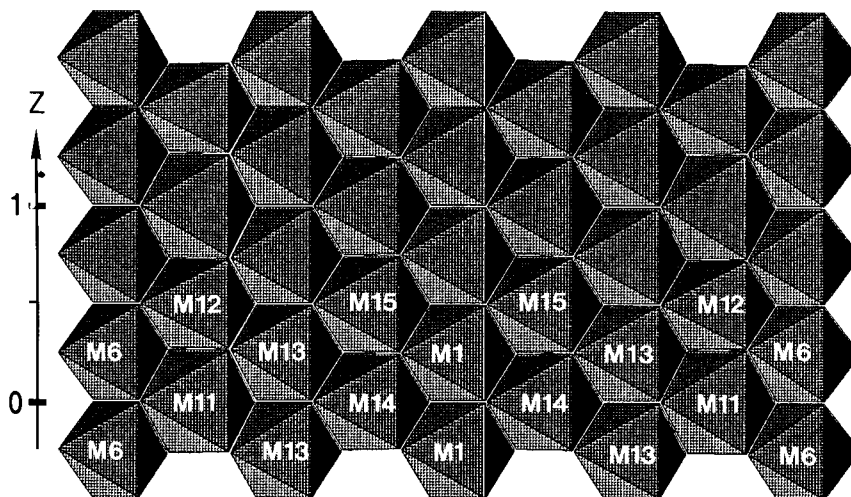


Fig. 5. Octahedral packing of the flat F wall of the takéuchiite structure. The c axis is pointing upwards. The manganese content of the metal positions M12, M14 and M15 is 100%, while that of M1, M6, M11 and M13 is 16, 6, 43 and 20% respectively.

remaining two columns of octahedra in the F wall, viz. the one with metal ions M11 and M12 and the other with ions M14 and M15, have a dominating Mn metal ion content. Thus, the Mn content at M12, M14 and M15 positions is 100% and that at M11 is 43%. The usual type of distorted octahedra oxygen coordination, due to the structural implication of the Jahn-Teller effect for Mn^{3+} , is pronounced around the pure Mn positions M12, M14 and M15. Thus, the coordination octahedra are formed by four shorter (about 1.97 Å) coplanar bonds and two longer (about 2.18 Å) ones. For the partially Mn occupied M11 position, the inverse distribution of bond distances is observed with four longer (about 2.20 Å) coplanar bonds and two shorter (1.99 Å) ones. It can be noted that the metal ion composition distribution of the columns in the F wall predicted by Takéuchi (1978), viz. a central column (M1) with dominating Mn content, is not obeyed in the present structure. In fact, the central column, as discussed above, has a dominating Mg content (84%).

The corrugated C wall of the zig-zag chain obtained when omitting the single S columns (see above) is shown in Figure 5 together with the labels of the metal ions. The oxygen octahedra formed around the metal ions M3, M8, M10 and M12 are considerably smaller in the c direction, compared to those around the M2, M7, M9 and M11. All these smaller octahedra contain 100% Mn. The octahedron around M12, which also is a member of the flat F wall has been described earlier. The distribution of the bond

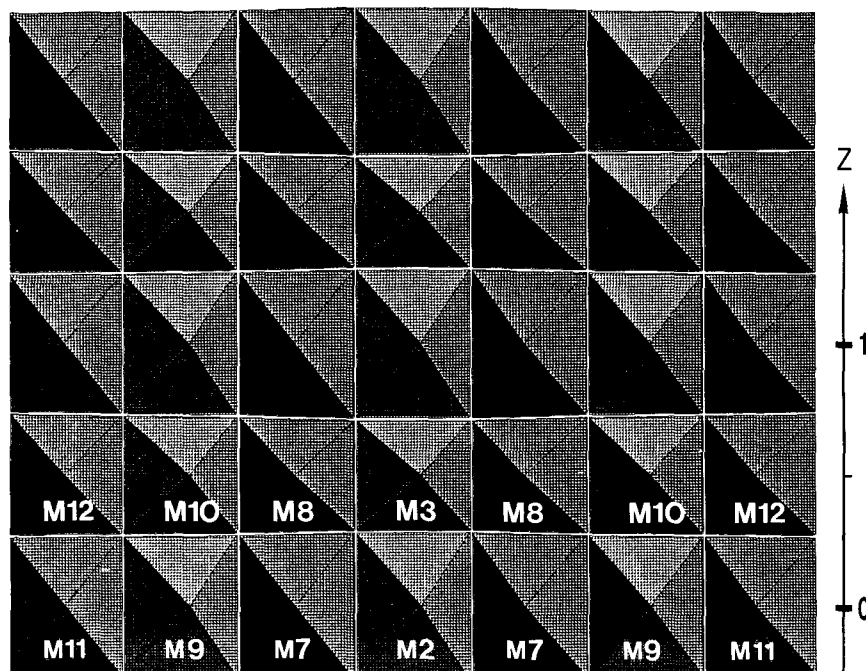


Fig. 6. Octahedral packing of the C wall of the takéuchiite structure. The c axis is pointing upwards. Note, that the M3, M8, M10 and M12 metal positions contain 100% Mn^{3+} .

distances in the M3, M8 and M10 octahedra are typical for Mn^{3+} , with four shorter coplanar bonds (about 1.91 Å) and two longer bonds (ranging from 2.16 to 2.27 Å). The longer bonds all extend out of the walls. The edgesharing between the MnO_6 octahedra thus occur in the planes with the short Mn-O bonds and gives rise to short Mn...Mn distances of about 2.7 Å. Due to the small size of this row of MnO_6 octahedra, the neighbouring row of octahedra formed around the metal ions M2, M7, M9 and M11 become distorted in the c direction. As seen in Figure 6 this distortion gradually increases towards the center of the wall. In this way the central octahedra (around M2 and M7) become rather large. A similar type of distortion also occurs in the F wall of orthopinakiolite (cf. Fig. 7). In orthopinakiolite, Takéuchi et al. (1978) used a structural model where the center octahedron of the F wall was only partially occupied (60%), while the metal position of the neighbouring octahedron was disordered (three alternative positions). In the present study the structural refinement indicated that the metal ion M2 in the central octahedron was disordered into mainly two positions. The short distance (1.186 Å) thus obtained between these M2 positions and that of the neighbouring metal M7 in-

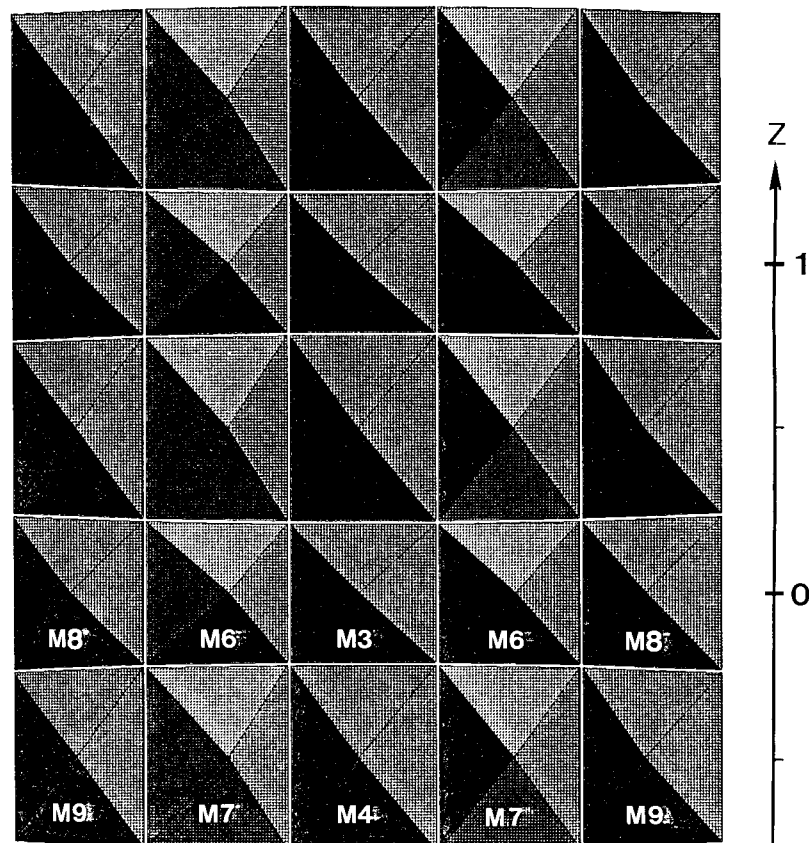


Fig. 7. Octahedral packing of the C wall of the orthopinakiolite (Takéuchi et al., 1978) structure. The c axis is pointing upwards. Note, that the M3, M6 and M8 metal positions contain 100% Mn^{3+} .

indicates that the disorder in this region of the structure extends also over the M7 position. A difference electron density map calculated without the contributions from the M2 and M7 metal ions (cf. Fig. 8) supports a rather continuous distribution of the metal ions positions in this region.

The composition of takéuchiite as calculated from the refined occupancies becomes $\text{Mg}_{1.71}\text{Mn}_{1.29}\text{BO}_5$. As mentioned above the Fe content of the composition found by microprobe analysis ($\text{Mg}_{1.59}\text{Mn}_{1.20}\text{Fe}_{0.19}\text{BO}_5$) was treated as Mn due to the similarity between the scattering factors of Mn and Fe. In view of the uncertainty of the microprobe analysis and of the refined occupancies this agreement is acceptable. With the assumption that all metal positions with 100% occupancy

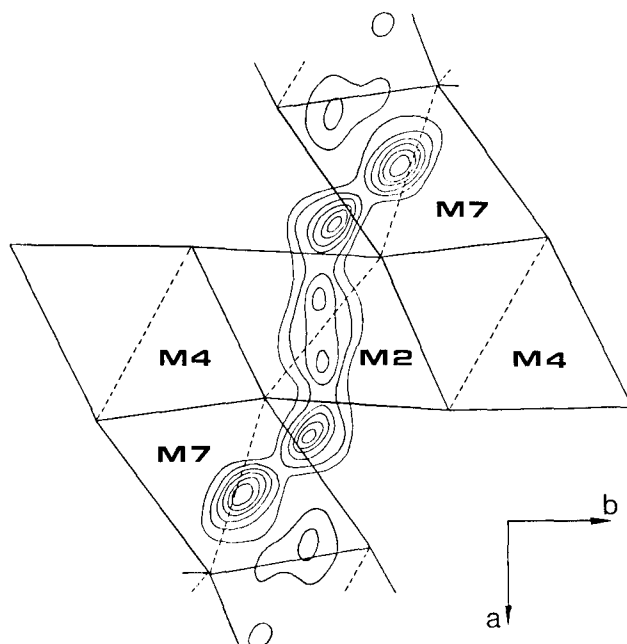


Fig. 8. Difference electron density map, in the plane $z = 0$ of takéuchiite, when omitting the M2 and M7 atomic positions from the structure factor calculation. For clarity, the oxygen coordination octahedra are outlined. Contours, indicating positive electron density, are drawn in steps of $3 e^-/\text{Å}^3$.

(M3, M8, M10, M12, M14 and M15) contain Mn^{3+} , which as discussed above agrees with the metal oxygen bond length distributions, the formal charge of the metal ion content $\text{Mg}_{1.71}^{2+}\text{Mn}_{0.37}^{2+}\text{Mn}_{0.92}^{3+}$ becomes + 6.92. This value is very close to the charge + 7.0 required for electroneutrality.

Acknowledgements. The availability of the Philips EM 430 electron microscope was made possible through grants from the Danish Research Councils SNF and STVF. One of the authors (J.-O. Bovin) is indebted to the Technical University of Denmark for financial support to maintain a position as visiting professor.

References

- Andersson, S., Hyde, B.: Twinning on the unit cell level as a structure building operation in the solid state. *J. Solid State Chem.* **9** (1974) 92–101.
- Bovin, J.-O., O'Keeffe, M.: Takéuchiite, a new oxyborate mineral from Långban, Sweden. *Am. Mineral.* **65** (1980) 1130–1133.
- Bovin, J.-O., O'Keeffe, M.: Electron microscopy of oxyborates. III. On the structure of takéuchiite. *Acta Crystallogr.* **A37** (1981 a) 42–46.

- Bovin, J.-P., O'Keeffe, M.: Electron microscopy of oxyborates. I. Defect structures in the minerals pinakiolite, ludwigite, orthopinakiolite and takéuchiite. *Acta Crystallogr.* **A37** (1981b) 28–45.
- International Tables for X-Ray Crystallography*, Vol. IV, Birmingham: Kynoch Press (1974).
- Moore, P., Araki, T.: Pinakiolite $\text{Mg}_2\text{MnO}_2\text{BO}_3$, warwickite $\text{Mg}(\text{Mn}_{0.5}\text{Ti}_{0.5})\text{OBO}_3$, weightmannite $\text{Mg}_5\text{O}(\text{OH})_5\text{BO}_3 \cdot \text{H}_2\text{O}$: Crystal structure of complex 3 Å wallpaper structure. *Am. Mineral.* **59** (1974) 985–1004.
- Norrestam, R.: Computer graphics of polyhedral packing. *Acta Crystallogr.* **A40** (1984) 438.
- Sheldrick, G. M.: *SHELX-76*. Program for Crystal Structure Determination. University of Göttingen (1976).
- Takéuchi, Y.: Complex structure of minerals. *Recent Prog. Nat. Sci. Jpn* **3** (1978) 153–181.
- Takéuchi, Y., Haga, N., Kato, T., Miura, Y.: Orthopinakiolite, $\text{Me}_{2.95}\text{O}_2\text{BO}_3$: Its crystal structure and relationship to pinakiolite, $\text{Me}_{2.90}\text{BO}_5$. *Can. Mineral.* **16** (1978) 475–485.
- Takéuchi, Y., Watanabé, T., Ito, T.: The crystal structures of warwickite, ludwigite and pinakiolite. *Acta Crystallogr.* **3** (1950) 98–107.